

RESEARCH ARTICLE

# Eocene Paleoclimatic Implications in the Bayat Basin Based on Nannofossil Distribution

Muhammad Rifa'i<sup>1</sup>, Siti Umiyatun Choiriah<sup>1\*</sup>, Akmaluddin<sup>2</sup>

<sup>1</sup> Department of Geology Engineering, Faculty of Mineral Technology, UPN "Veteran" Yogyakarta, Depok, Sleman, Yogyakarta 55283, Indonesia

<sup>2</sup> Department of Geological Engineering, Faculty of Engineering, Universitas Gadjah Mada, Sleman 55281, Yogyakarta, Indonesia

\* Corresponding author : umiyatunch@upnyk.ac.id  
Tel.: +62 856-4363-6379  
Received: Apr 07, 2026; Accepted: May 11, 2026.  
DOI: 10.25299/jgeet.2026.11.02.27718

## Abstract

The Middle–Late Eocene represents a critical interval of greenhouse climate evolution following the Early Eocene Climatic Optimum (EECO), yet quantitative paleoclimate records from low-latitude Southeast Asia remain scarce. This study presents a multi-proxy calcareous nannofossil-based reconstruction of surface-water conditions from the Gamping–Wungkal Formation in the Bayat Basin, southern Java. Detailed stratigraphic logging and systematic sampling along a 60 m section were combined with quantitative assemblage analysis and Scanning Electron Microscope validation. Biostratigraphic evaluation assigns the studied interval to the NP17 zone (Middle–Late Eocene). Paleoclimatic reconstruction integrates the Reticulofenestra Size Ratio (RSR), Warm-Water Index (WWI), Discoaster Abundance Ratio (DAR), and total Reticulofenestra abundance. Assemblages are dominated by medium- to large-sized Reticulofenestra and persistent Discoaster occurrences, indicating warm, oligotrophic, and stratified surface-water conditions. Despite global post-EECO cooling trends documented in mid- and high-latitude records, the Bayat data suggest sustained tropical greenhouse conditions during NP17. These findings are consistent with emerging evidence of latitudinal variability in Eocene climate evolution and establish the Bayat Basin as an important low-latitude archive for evaluating Paleogene greenhouse dynamics in Southeast Asia.

**Keywords:** Bayat, Eocene, Gamping Wungkal, Nannofossil, Paleoclimate

## 1. Introduction

### 1.1 Regional Physiography

The Bayat area lies within the Southern Mountains Zone of Central Java, a structurally complex region formed by interactions between carbonate platforms, metamorphic basement, and volcanic sequences. This structural complexity has significantly influenced topography, with differential erosion producing undulating hills and ridges (Surono, 2009). Recent geomorphological studies of Central Java demonstrate that tectonic uplift and erosion associated with arc-continent interactions, as well as variations in lithological resistance, strongly influence hill-valley morphology in similar Central Java terrains, highlighting the region's active landscape development (Hidayat et al., 2021).

### 1.2 Regional Geological Structure

Tectonically, the Bayat area lies within the northern segment of the Javanese magmatic arc, part of the broader Sunda Arc system, which developed as a consequence of the long-term subduction of the Indo-Australian Plate beneath the Eurasian Plate since the Late Cretaceous (Gallagher et al., 2024; Hall, 2011). This convergent margin generated regional deformation characterized by thrust faults, strike-slip faults, and fold belts trending predominantly northwest–southeast to east–west, which control lithological distribution and structural grain across southern Java. Recent tectonic syntheses further demonstrate that Java's Paleogene evolution was influenced by arc migration, slab rollback, and back-arc basin dynamics (Luan and Lunt, 2021; Lunt and Luan, 2023), processes that contributed to uplift and exhumation of Eocene carbonate units such as the Gamping–Wungkal Formation in the Bayat Basin. This structural

framework provides the tectonic basis for the present-day exposure of Eocene successions and enables detailed stratigraphic and micropaleontological investigation (Figure 1).

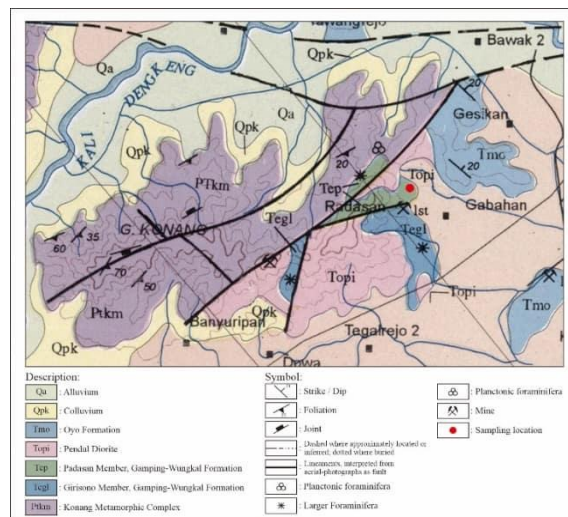


Fig. 1. Geological map of the study area (Samudra and Sutisna, 1992).

### 1.3 Regional Stratigraphy

The stratigraphy of the Bayat area comprises a sequence of major lithostratigraphic units from oldest to youngest (Figure 2), including the Bayat Metamorphic Complex (pre-Tertiary basement), the Gamping–Wungkal Formation (Eocene shallow-marine carbonates and claystones), the Kebo-Butak Formation (Oligocene–Miocene volcanic and

sedimentary rocks), and unconsolidated Quaternary volcanic deposits (Mulyaningsih, 2016; Surono, 2009).

Regional sedimentation patterns across Java demonstrate that Paleogene carbonate successions, like the Gamping-Wungkal, formed within broader tectono-stratigraphic frameworks influenced by dynamic subsidence, sea-level changes, and provenance shifts (Luan and Lunt, 2021; Lunt and Luan, 2023). Research on carbonate and siliciclastic deposition in eastern Java and adjacent basins underscores the role of tectonics in controlling accommodation space and sediment basin fill across the Eocene–Miocene (Gallagher et al., 2024; Hall, 2019), which supports interpretations of stratigraphic architecture in the Bayat region.

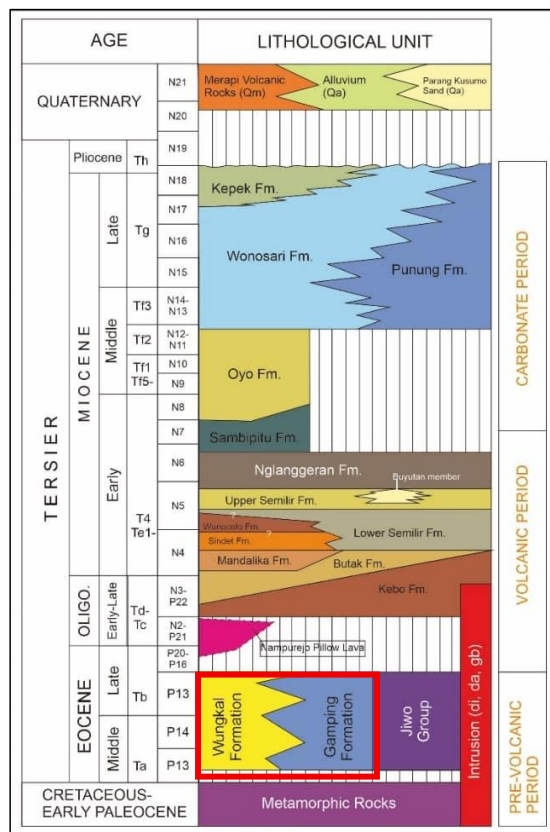


Fig. 2. Regional stratigraphy of the Southern Mountain (Surono, 2009).

The Gamping-Wungkal Formation itself contains abundant Eocene coccoliths and other microfossils, with taxa such as *Reticulofenestra* and *Coccolithus* indicating deposition in a shallow-marine environment favorable for preservation of calcareous nannofossils (Novita et al., 2014; Umiyatun et al., 2006).

The Gamping–Wungkal Formation represents one of the Paleogene carbonate successions exposed within the Southern Mountains Zone of Java. Carbonate deposition during the Eocene in Southeast Asia commonly occurred in shallow marine environments associated with carbonate platforms that formed along the margins of Sundaland under tropical greenhouse conditions. These carbonate systems were strongly influenced by the tectonic evolution of the Sunda Arc, where regional subsidence and volcanic arc activity periodically controlled sediment supply and accommodation space for carbonate accumulation. Consequently, mixed carbonate and fine-grained siliciclastic deposits such as micritic limestone, marl, and claystone are commonly preserved in arc-related basins of Southeast Asia. Similar carbonate platform developments during the Eocene have been documented in several Tethyan and Southeast

Asian regions, where carbonate sedimentation occurred in warm shallow marine environments connected to open-ocean circulation (Fang et al., 2024; Luan and Lunt, 2021; Lunt, 2023).

## 1.4 Paleoclimate Based on Nannofossil

### 1.4.1 Nannofossil

Nannofossils are widely recognized as key indicators for Paleogene biostratigraphy due to their rapid evolutionary rates and sensitivity to environmental changes (Agnini et al., 2014). Previous studies in the Bayat area (Umiyatun et al., 2006) reported Paleogene taxa indicating an NP18–NP19 age range.

Furthermore, recent studies in Indonesia demonstrate that quantitative nannofossil distributions provide reliable proxies for reconstructing paleoceanographic conditions, including temperature, stratification, and productivity (Farida et al., 2024; Ratumanan et al., 2023). The integration of taxonomic composition and abundance patterns in this study therefore provides a robust basis for interpreting Eocene shallow-marine conditions in the Bayat Basin.

### 1.4.2 Paleoclimate

Paleoclimatic interpretation using calcareous nannofossils is commonly based on taxonomic composition, relative abundance, and quantitative indices (Agnini et al., 2014; Blaj et al., 2023; Ma et al., 2024; Menini et al., 2021).

Nannofossil taxa exhibit distinct ecological preferences. Variations in the size structure of *Reticulofenestra* reflect nutrient availability and upper-ocean conditions. Larger morphotypes are typically associated with oligotrophic and stratified waters, whereas smaller morphotypes indicate increased nutrient supply (Judd et al., 2022; Ma et al., 2024; Menini et al., 2021).

Similarly, Discoaster abundance is widely interpreted as an indicator of warm, oligotrophic, and stratified surface waters, particularly in low-latitude greenhouse settings (Judd et al., 2022; Ma et al., 2024).

Quantitative nannofossil-based indices such as *Reticulofenestra* Size Ratio (RSR), Warm-Water Index (WWI), Discoaster Abundance Ratio (DAR), and the relative abundance of *Reticulofenestra* are widely applied in Paleogene paleoceanographic studies. However, most studies do not define universal threshold values to classify these parameters into “low”, “moderate”, or “high” categories. Instead, interpretations are typically based on relative variations within individual stratigraphic sections and their ecological significance (Judd et al., 2022; Ma et al., 2024; Menini et al., 2021).

Therefore, in this study, the classification of parameter values (e.g., low or high RSR, WWI, and DAR) is interpreted in a relative sense based on internal variations between samples and supported by ecological relationships between nannofossil assemblages and surface-water conditions.

### 1.4.3 *Reticulofenestra* Size Ratio

The *Reticulofenestra* Size Ratio (RSR) was calculated as the ratio between small-sized individuals (<5 μm) and large-sized individuals (>7 μm). Variations in the size structure of *Reticulofenestra* are widely recognized as reflecting changes in surface-water nutrient availability, water-column stability, and broader paleoceanographic conditions during the Paleogene (Agnini et al., 2014; Ma et al., 2024). Quantitative morphometric studies demonstrate that dominance of large-sized morphotypes is typically associated with oligotrophic, stratified, and relatively stable surface waters. In contrast, increased proportions of small-sized morphotypes correspond

to enhanced nutrient supply and elevated productivity (Judd et al., 2022; Menini et al., 2021). Such size-structured assemblage shifts have been documented in Middle–Late Eocene records and are interpreted as reflecting regional adjustments in upper-ocean trophic conditions (Hollis et al., 2022).

#### 1.4.4 Warm-Water Index

The Warm-Water Index (WWI) was calculated based on the relative abundance of warm-water and large-sized taxa, namely *Coccolithus pelagicus* and *Reticulofenestra umbilicus*, which are commonly associated with relatively stable and stratified surface-water conditions during the Paleogene. Variations in the abundance of large reticulofenestrads and coccolith-bearing taxa have been interpreted as reflecting upper-ocean stability and nutrient limitation in low-latitude Eocene settings (Hutchinson et al., 2021; Ma et al., 2024).

#### 1.4.5 Discoaster Abundance Ratio

The Discoaster Abundance Ratio (DAR) reflects the relative proportion of Discoaster within the assemblage and is commonly used as a proxy for warm and oligotrophic surface-water conditions (Judd et al., 2022).

Previous studies have demonstrated that fluctuations in *Discoaster* abundance can be used to track variations in surface-water stability and ecological structure of coccolithophore communities. Increased representation of *Discoaster* is often interpreted as reflecting enhanced stratification and reduced nutrient supply, whereas reduced abundance may indicate relatively more dynamic or nutrient-influenced conditions (Judd et al., 2022; Menini et al., 2021).

#### 1.4.6 Total *Reticulofenestra* Abundance

The relative abundance of *Reticulofenestra* is widely used as an indicator of paleoceanographic conditions in Paleogene marine environments. This genus represents one of the most dominant coccolithophore groups in low- to mid-latitude settings and exhibits strong sensitivity to changes in nutrient availability, surface-water stratification, and productivity (Agnini et al., 2014; Ma et al., 2024).

High relative abundance of *Reticulofenestra* is commonly associated with oligotrophic and stratified surface waters, where stable conditions favor continuous coccolithophore production. Conversely, reduced abundance may indicate increased nutrient input, higher productivity, or more dynamic water-column conditions that disrupt coccolithophore dominance (Judd et al., 2022).

### 1.5 Background

Reconstruction of the Eocene paleoclimate is a major topic in modern geology, as this interval witnessed significant global climate variability, including extreme warming during the Eocene Climatic Optimum and subsequent cooling toward the Eocene-Oligocene transition (Hollis et al., 2022; Hutchinson et al., 2021; Pearson et al., 2015; Westerhold et al., 2021). Recent syntheses emphasize that Middle–Late Eocene climate evolution involved complex feedbacks among atmospheric CO<sub>2</sub>, fluctuations in carbonate compensation depth, and ocean productivity, highlighting the importance of integrating regional marine archives into globally calibrated chronostratigraphic frameworks (Westerhold et al., 2024).

Recent high-resolution Paleogene studies demonstrate that climate evolution during the late Paleogene was characterized by complex regional variability rather than uniform global change. Integrated stratigraphic and geochemical data from continental margin successions reveal

short-lived cooling phases linked to carbon-cycle perturbations and atmospheric CO<sub>2</sub> fluctuations (Hollis et al., 2022; Westerhold et al., 2021). Across the Eocene–Oligocene Transition (EOT), coupled isotopic and calcareous nanofossil records document major paleoceanographic reorganization, including shifts in carbonate chemistry, productivity structure, and preservation dynamics (Hutchinson et al., 2021). These findings highlight that surface-water ecological responses may vary regionally and emphasize the importance of well-constrained marine archives for refining paleoclimate reconstructions.

In Indonesia, however, paleoclimate data based on nanofossils remain limited, particularly in central Java, where numerous Paleogene rock units are well exposed. One of these units is the Gamping-Wungkal Formation, which has been interpreted as a shallow-marine carbonate deposit (Suroño, 2009) of Middle to Late Eocene age (Umiyatun et al., 2006) and represents a potentially important archive of paleoenvironmental change in the ancient tropical region.

Nanofossils are effective paleoclimate indicators due to their rapid evolutionary rates, broad geographic distribution, and sensitivity to changes in temperature, nutrient availability, and water-column stratification (Agnini et al., 2017). Indices such as *Discoaster* abundance, size variations of the genus *Reticulofenestra*, and changes in *Helicosphaera* abundance have been widely applied to reconstruct Paleogene shallow-marine climate dynamics. Recent Paleogene studies in Indonesia highlight the importance of nanofossil-based approaches for paleoenvironmental interpretation, as demonstrated by studies of the Tonasa Formation (Farida et al., 2024), the Nanggulan Formation (Jatiningrum et al., 2022), and the Elat Formation in Maluku (Ratumanan et al., 2023).

Previous studies in Bayat (Umiyatun et al., 2006) documented the presence of Eocene nanofossils, including *Criboecentrum reticulatum*, *Discoaster saipanensis*, *Discoaster barbadiensis*, *Discoaster deflandrei*, *Reticulofenestra umbilica*, *Reticulofenestra hampdenensis*, *Helicosphaera compacta*, *Helicosphaera euphratis*, *Ericsonia formosa*, *Zyghrablithus bijugatus*, *Sphenolithus moriformis*, and *Sphenolithus pseudoradians*. However, no systematic attempt has been made to relate their distribution to regional paleoclimatic conditions. Previous studies documented only taxonomic occurrence and zonation. This research is the first to quantitatively integrate assemblage structure with climate-sensitive indices to reconstruct paleoceanographic conditions.

This study aims to fill this gap by analyzing nanofossil distribution in the study area, which lies within the Paleogene basin of the Southern Mountains of Java. The results are expected to contribute to the reconstruction of the Eocene paleoclimate in Java and to serve as a reference for future studies in stratigraphy, carbonate sedimentology, and micropaleontology.

### 1.5 Objectives

The objectives of this study are to:

1. Identify the distribution of nanofossils in the claystone of the Gamping-Wungkal Formation within the study area.
2. Determine the relative age based on nanofossil zonation.
3. Interpret Eocene paleoclimate conditions based on nanofossil abundance and diversity.

### 2. Material And Method

The study area is located at Watuprahu, Dusun III, Gunung Gajah, Bayat, Klaten, Central Java, Indonesia, with UTM coordinates X = 463961 and Y = 9141582 (Zone 49S)

(Figure 3). Stratigraphic measurements and sampling were conducted on well-exposed claystone outcrops with high potential for nanofossil occurrence.

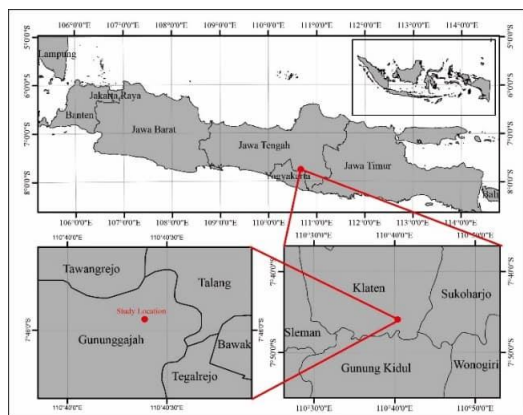


Fig. 3. Index map of the study area.

The research methods applied in this study are described as follows:

#### A. Measured Stratigraphic Section

A stratigraphic section approximately 60 m thick was measured in detail along the Watuprahu outcrop using a measuring tape and a geological compass. Lithological variations, sedimentary structures, and sampling positions were systematically recorded along the section. The measured stratigraphic profile, including lithological succession and sampling locations, is presented in Figure 7.

#### B. Sampling

Six claystone samples were collected from the measured stratigraphic section using a representative sampling approach. Sampling was conducted at regular stratigraphic intervals of several meters along the measured section, ensuring that each sample reflects variations in lithology and stratigraphic position. The selected samples specifically target claystone horizons considered suitable for nanofossil analysis. Each sample was systematically labeled, and its exact stratigraphic position was recorded during fieldwork.

#### C. Smear Slide Preparation

Fine-grained claystone samples were gently crushed to obtain a fine powder, suspended in distilled water, mounted on glass slides, and heated to fix the material.

#### D. Polarizing Light Microscope Analysis

Nanofossils were observed using a polarizing light microscope with a 40× objective magnification under both plane-polarized and cross-polarized light. Taxonomic identification was based on morphological characteristics and optical properties of the nanofossils, following standard taxonomic frameworks established by Martini (1971), Agnini et al. (2017), and Raffi et al. (2022).

Quantitative analysis was conducted using the random field counting method. Each smear slide was examined in four randomly selected fields of view. The total number of counted nanofossil specimens per sample ranged from approximately 30 to 50 individuals. Nanofossil abundance was expressed as relative abundance (%), calculated as the proportion of individuals of a given taxon relative to the total number of nanofossil individuals counted on each slide.

#### E. Scanning Electron Microscope (SEM) Analysis

SEM analysis was performed to obtain high-resolution images of nanofossils, confirm taxonomic identification, and document preservation states. SEM images were used as supporting data to validate observations obtained from polarizing light microscopy.

#### F. Relative Age Determination and Paleoclimate Analysis

Relative age determination was conducted based on Paleogene nanofossil zonation following Martini (1971). Paleoclimate interpretation was achieved by integrating several quantitative parameters commonly applied in calcareous nanofossil studies (Agnini et al., 2014; Ma et al., 2024; Menini et al., 2021), including:

##### 1) *Reticulofenestra* Size Ratio (RSR)

$$RSR = \frac{N_{small\ Reticulofenestra}}{N_{large\ Reticulofenestra}} \dots \dots \dots (1)$$

##### 2) Warm-Water Index (WWI)

$$WWI (\%) = \frac{N_{warm\ water\ taxa}}{N_{total\ nanofossil}} \times 100 \dots \dots \dots (2)$$

##### 3) *Discoaster* Abundance Ratio (DAR)

$$DAR (\%) = \frac{N_{Discoaster}}{N_{total\ nanofossil}} \times 100 \dots \dots \dots (3)$$

##### 4) Total *Reticulofenestra* abundance

$$Reticulofenestra (\%) = \frac{N_{total\ Reticulofenestra}}{N_{total\ nanofossil}} \times 100 (4)$$

These parameters were applied to reconstruct variations in sea surface temperature, water-column stability, and surface-water productivity during the Eocene. The *Reticulofenestra* Size Ratio (RSR) is primarily used as an indicator of nutrient availability and productivity, where higher proportions of small-sized morphotypes generally reflect increased nutrient supply and more eutrophic conditions, while dominance of larger morphotypes indicates oligotrophic environments.

The Warm-Water Index (WWI) serves as a proxy for sea surface temperature, as it is based on the relative abundance of warm-water taxa such as *Coccolithus pelagicus* and *Reticulofenestra umbilicus*, which are typically associated with elevated temperatures in low-latitude marine settings.

The *Discoaster* Abundance Ratio (DAR) is widely interpreted as an indicator of water-column stability and stratification, as *Discoaster* taxa are commonly associated with warm, stratified, and oligotrophic surface waters. Higher DAR values therefore reflect increased stratification and reduced vertical mixing.

Finally, total *Reticulofenestra* abundance provides additional insight into overall surface-water conditions, including productivity levels and ecological dominance within the nanoplankton community. These interpretations are based on established ecological relationships between nanofossil assemblages and surface-oceanographic conditions (Agnini et al., 2014; Ma et al., 2024; Okada and Honjo, 1973).

### 3. Result and Discussions

The stratigraphy of the Bayat area is generally composed of a pre-Tertiary metamorphic rock complex, overlain by carbonate-clastic units that are regionally correlated with the Eocene Gamping-Wungkal Formation (Surono, 2009). However, at the local scale, contacts between units are indistinct, irregular, and challenging to trace laterally. Consequently, age determination of the stratigraphic units relies heavily on nanofossil biostratigraphy. The outcrop conditions and sampling traverse used for systematic claystone sampling along a 60 m measured section are shown in Figure 4.



Fig. 4. Outcrop photograph of the sampling location in the study area. The outcrop extends from south to north and has an approximate length of 60 m. Points of interest include claystone, graphite intercalations, and limestone layers, with evidence of

landslide deposits observed in the northern part of the outcrop. The white dashed line indicates the sampling traverse.



Fig. 5. Limestone unit in the study area.

### 3.1 Limestone Unit of the Gamping-Wungkal Formation

Along the measured section, limestone occurs only as isolated and discontinuous exposures (Figure 7), characterized by dark black coloration and a micritic texture (Figure 5). The irregular distribution of these limestones suggests that they represent remnants of the carbonate facies of the Gamping-Wungkal Formation that have undergone intense deformation and erosion. Regionally, the carbonate unit of the Gamping-Wungkal Formation is assigned to the Middle-Late Eocene (Surono, 2009) and is commonly associated with microfossil-rich shale.

### 3.2 Claystone Unit of the Gamping-Wungkal Formation

Claystone is the dominant lithological unit and the primary focus of this study (Figure 7). The claystone exhibits color variations ranging from reddish brown and dark brown to gray, reflecting differences in organic matter content and redox conditions (Figure 6a). Its widespread distribution and association with sandstone support its assignment to the Gamping-Wungkal Formation, within which graphite intercalations are locally observed (Figure 6b). Due to unclear stratigraphic relationships and the absence of well-defined contacts in the field, age determination of this unit is based on nanofossil analysis.



Fig. 6. Field photographs of the Claystone unit of the Gamping-Wungkal Formation in the study area. (a) claystone unit showing massive texture and brown to gray coloration; (b) graphitic claystone characterized by darker color and graphite-rich layers.

The lithological association of micritic limestone and claystone observed within the studied section suggests sedimentation under relatively low-energy marine conditions. Micritic carbonate typically forms through the accumulation of fine carbonate mud produced by planktonic organisms and microbial processes in calm-water settings. In contrast, the presence of claystone indicates the contribution of fine terrigenous or hemipelagic material settling through the water column. Such lithological characteristics are commonly associated with outer neritic to open-shelf environments along carbonate platform margins. In tropical greenhouse

intervals such as the Middle–Late Eocene, these environments supported high coccolithophore productivity, leading to the accumulation of calcareous nanofossils within fine-grained marine sediments (Ghandour et al., 2023; Villa et al., 2021).

GEOLOGIC AGE	LITHOSTRATIGRAPHIC UNIT	THICKNESS (METERS)	LITHOLOGY	DESCRIPTION
EPOCH	FORMATION	ROCK UNIT		
NP17 (Middle-Late Eocene)	Gamping-Wungkal	Claystone	3,73	Claystone; grayish brown (fresh); dark brown (weathered); clay sized (<0.004 mm); m: clay sized material; parallel laminated
		Claystone	2,14	Graphitic claystone; dark gray (fresh); black (weathered); clay sized (<0.004 mm); m: clay sized material; parallel laminated
		Claystone	12,23	Claystone; grayish brown (fresh); dark brown (weathered); clay sized (<0.004 mm); m: clay sized material; parallel laminated
		Limestone	1,15	Foraminiferal limestone; dark gray (fresh); black (weathered); medium to coarse sand sized (0.25–1 mm); poorly sorted; matrix supported; composed by A: foraminifera, liliac fragment, microlite; M: calcite; C: carbonate; massive
		Claystone	14,15	Claystone; reddish brown (fresh); dark brown (weathered); clay sized (<0.004 mm); m: clay sized material; parallel laminated

Fig. 7. Stratigraphy of the study area.

As shown in Figure 7, the measured stratigraphic section represents the corrected thickness of exposed lithological units rather than the total lateral extent of the outcrop, which reaches approximately 60 m. Vertical variations within the studied interval indicate relatively stable depositional conditions during the accumulation of the claystone-dominated succession of the Gamping–Wungkal Formation. The persistence of fine-grained lithologies and the absence of significant changes in sedimentary facies suggest continuous marine sedimentation without major shifts in depositional energy or water depth.

Sampling locations are distributed along the measured section and are indicated in Figure 7, primarily targeting claystone intervals suitable for nanofossil analysis. Minor fluctuations observed in the relative abundance of calcareous nanofossils (Table 2) likely reflect subtle variations in surface-water productivity rather than major environmental changes. Similar stratigraphic patterns have been documented in other Eocene marine successions where stable greenhouse climatic conditions promoted persistent coccolithophore productivity and continuous pelagic carbonate sedimentation (Raffi et al., 2022; Villa et al., 2021).

### 3.3 Nanofossil

Based on nanofossil analysis of the study area, the fossil assemblages exhibit compositional and abundance variations consistent with Martini's (1971) zonation scheme. All six samples are characterized by the dominance of *Reticulofenestra bisecta*, *Reticulofenestra erbae*, *Coccolithus pelagicus*, and the continuous occurrence of *Discoaster barbadiensis*, indicating assignment to the NP17 zone (Middle–Late Eocene) (Table 1). The relative abundance of nanofossil taxa in each sample is summarized in Table 2. Taxonomic identification and preservation assessment were conducted using light microscopy and SEM observations; representative photomicrographs are presented in Figure 8 and SEM images in Figure 9.

Table 1. Relative-age zonation table for the study area based on nannofossil distribution.

Sample	Eocene					Oligocene					Age						
	10	11	12	13	14	15	16	17	18	19	20	21	22	23	24	25	NP Zone
MR.01	[Horizontal line from 11 to 21]																<i>Coccolithus formosus</i>
	[Horizontal line from 10 to 21]																<i>Coccolithus pelagicus</i>
	[Horizontal line from 15 to 21]																<i>Cyclicargolithus floridanus</i>
	[Horizontal line from 11 to 21]																<i>Discoaster barbadiensis</i>
	[Horizontal line from 10 to 21]																<i>Reticulofenestra bisecta</i>
	[Horizontal line from 17 to 21]																<i>Reticulofenestra erbae</i>
	[Horizontal line from 13 to 21]																<i>Reticulofenestra minuta</i>
	[Horizontal line from 14 to 17]																<i>Sphenolithus moriformis</i> <i>Sphenolithus spiniger</i>
MR.02	[Horizontal line from 11 to 21]																<i>Coccolithus formosus</i>
	[Horizontal line from 10 to 21]																<i>Coccolithus pelagicus</i>
	[Horizontal line from 15 to 21]																<i>Cyclicargolithus floridanus</i>
	[Horizontal line from 11 to 21]																<i>Discoaster barbadiensis</i>
	[Horizontal line from 12 to 16]																<i>Helicosphaera seminulum</i>
	[Horizontal line from 14 to 21]																<i>Reticulofenestra bisecta</i>
	[Horizontal line from 13 to 21]																<i>Reticulofenestra daviesii</i>
	[Horizontal line from 13 to 21]																<i>Reticulofenestra dictyoda</i>
	[Horizontal line from 17 to 21]																<i>Reticulofenestra erbae</i>
	[Horizontal line from 17 to 21]																<i>Reticulofenestra lockeri</i>
	[Horizontal line from 13 to 21]																<i>Reticulofenestra minuta</i>
	[Horizontal line from 15 to 21]																<i>Reticulofenestra umbilicus</i> <i>Sphenolithus furcatolithoides</i>
[Horizontal line from 14 to 17]																<i>Sphenolithus moriformis</i> <i>Sphenolithus spiniger</i>	
MR.03	[Horizontal line from 10 to 21]																<i>Coccolithus pelagicus</i>
	[Horizontal line from 15 to 21]																<i>Cyclicargolithus floridanus</i>
	[Horizontal line from 11 to 21]																<i>Discoaster barbadiensis</i>
	[Horizontal line from 17 to 21]																<i>Reticulofenestra bisecta</i>
	[Horizontal line from 17 to 21]																<i>Reticulofenestra erbae</i>
	[Horizontal line from 14 to 21]																<i>Reticulofenestra hampdenensis</i>
	[Horizontal line from 17 to 21]																<i>Reticulofenestra lockeri</i>
	[Horizontal line from 13 to 21]																<i>Reticulofenestra minuta</i>
	[Horizontal line from 15 to 21]																<i>Reticulofenestra reticulata</i>
	[Horizontal line from 11 to 24]																<i>Sphenolithus radians</i> <i>Sphenolithus spiniger</i>
MR.04	[Horizontal line from 10 to 21]																<i>Coccolithus pelagicus</i>
	[Horizontal line from 15 to 21]																<i>Coronocyclus nitescens</i>
	[Horizontal line from 15 to 21]																<i>Cyclicargolithus floridanus</i>
	[Horizontal line from 13 to 21]																<i>Discoaster saipanensis</i>
	[Horizontal line from 13 to 24]																<i>Discoaster tanii</i>
	[Horizontal line from 17 to 21]																<i>Reticulofenestra bisecta</i>
	[Horizontal line from 13 to 21]																<i>Reticulofenestra dictyoda</i>
	[Horizontal line from 17 to 21]																<i>Reticulofenestra erbae</i>
	[Horizontal line from 14 to 21]																<i>Reticulofenestra hampdenensis</i>
	[Horizontal line from 13 to 21]																<i>Reticulofenestra minuta</i>
	[Horizontal line from 15 to 17]																<i>Sphenolithus furcatolithoides</i>
	[Horizontal line from 10 to 21]																<i>Sphenolithus moriformis</i> <i>Sphenolithus radians</i> <i>Sphenolithus spiniger</i>
MR.05	[Horizontal line from 11 to 21]																<i>Coccolithus pelagicus</i>
	[Horizontal line from 11 to 21]																<i>Discoaster barbadiensis</i>
	[Horizontal line from 13 to 21]																<i>Discoaster saipanensis</i>
	[Horizontal line from 17 to 21]																<i>Reticulofenestra bisecta</i>
	[Horizontal line from 13 to 21]																<i>Reticulofenestra dictyoda</i>
	[Horizontal line from 17 to 21]																<i>Reticulofenestra erbae</i> <i>Reticulofenestra lockeri</i> <i>Reticulofenestra minuta</i>

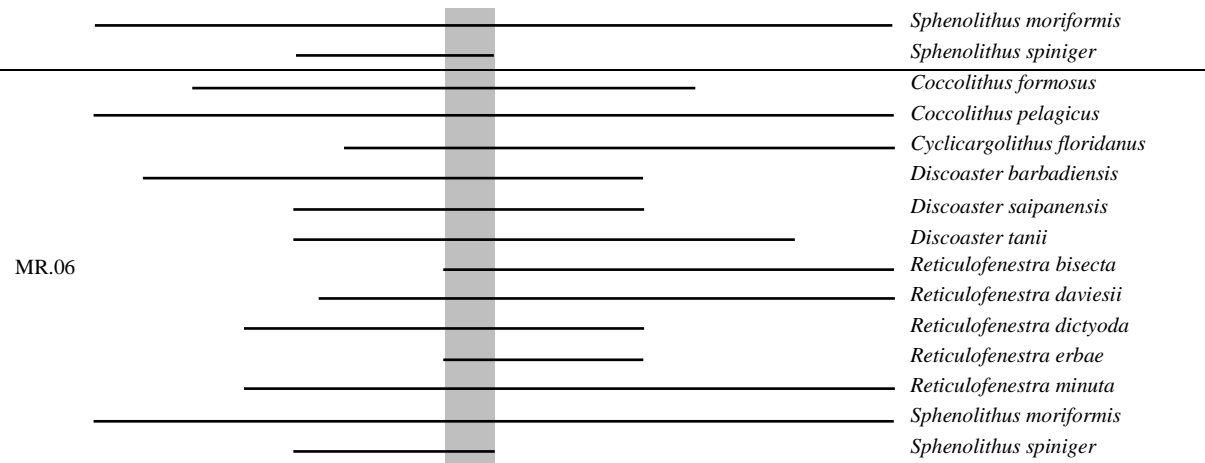


Table 2. Nannofossil abundance table of the study area.

Nannofossil	Sample					
	MR.01	MR.02	MR.03	MR.04	MR.05	MR.06
<i>Coccolithus formosus</i>	1	5				3
<i>Coccolithus pelagicus</i>	4	13	1	2	1	4
<i>Coronocyclus nitescens</i>				1		
<i>Cyclicargolithus floridanus</i>	4	4	1	2		4
<i>Discoaster barbadiensis</i>	2	2	1		1	6
<i>Discoaster saipanensis</i>				2	3	2
<i>Discoaster tani</i>				1		1
<i>Helicosphaera seminulum</i>		2				
<i>Reticulofenestra bisecta</i>	10	9	7	5	7	10
<i>Reticulofenestra daviesii</i>		1				2
<i>Reticulofenestra dictyoda</i>		3		1	1	4
<i>Reticulofenestra erbae</i>	12	7	10	10	6	14
<i>Reticulofenestra hampdenensis</i>			1	1		
<i>Reticulofenestra lockeri</i>		1	1		2	
<i>Reticulofenestra minuta</i>	3	5	1	2	2	4
<i>Reticulofenestra reticulata</i>			1			
<i>Reticulofenestra umbilicus</i>		1				
<i>Sphenolithus furcatolithoides</i>		1		1		
<i>Sphenolithus moriformis</i>	5	4		5	1	5
<i>Sphenolithus radians</i>			1	2		
<i>Sphenolithus spiniger</i>	4	1	1	2	1	5

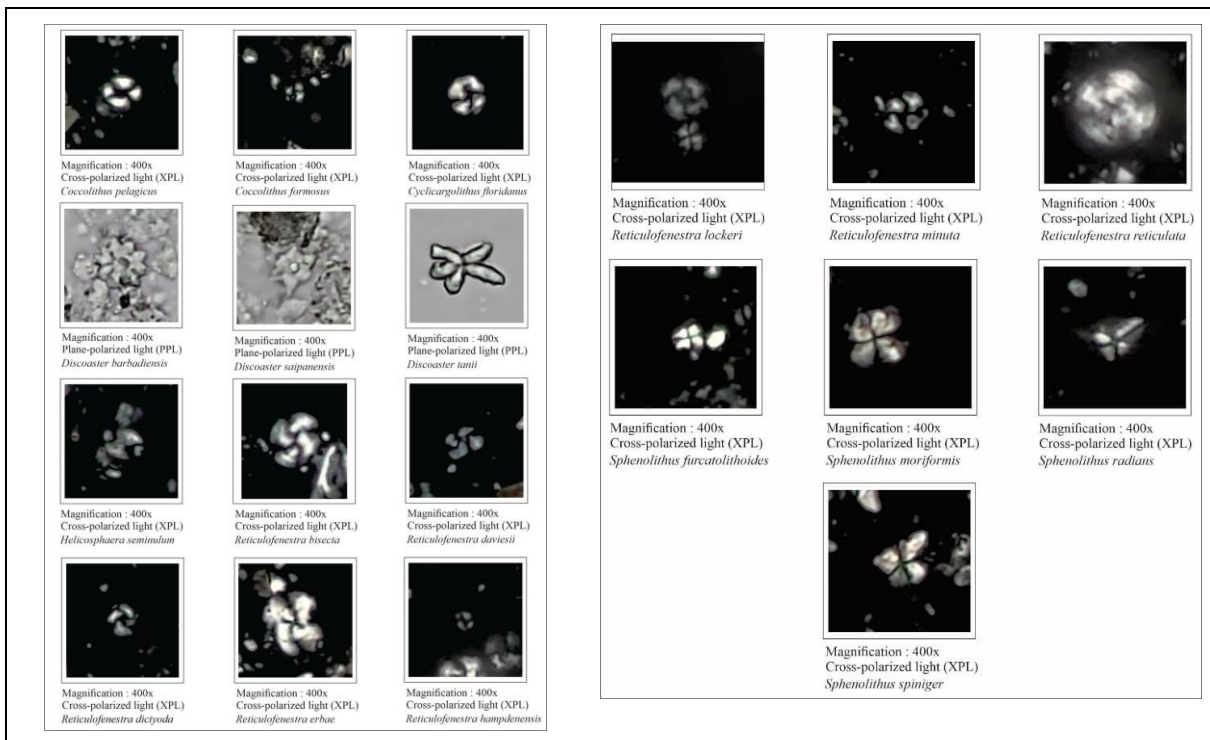


Fig. 8. Photomicrographs of nannofossil species from the study area were obtained using a polarizing microscope.

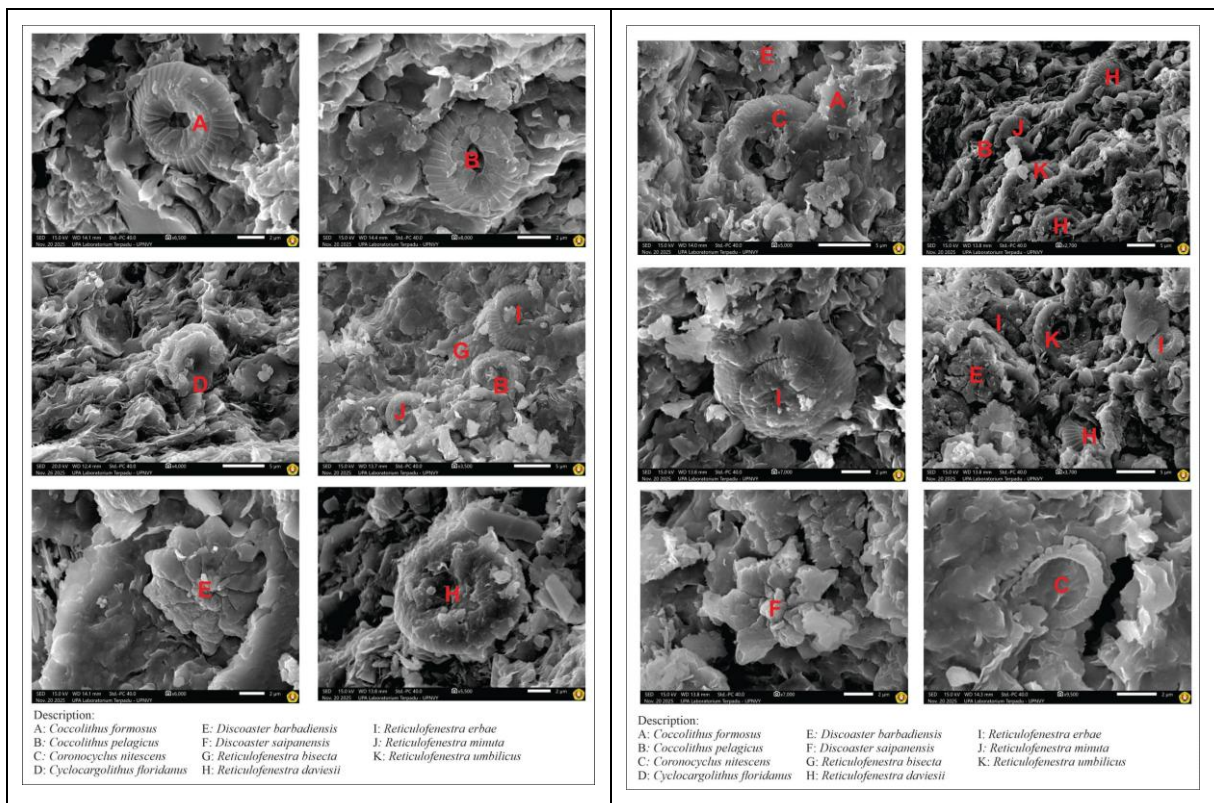


Fig. 9. Scanning Electron Microscope (SEM) images of nannofossil species from the study area.

### 3.4 *Reticulofenestra* Size Ratio (RSR)

Based on the abundance data of *Reticulofenestra* taxa (Table 2), all samples are dominated by large-sized species, including *Reticulofenestra dictyoda*, *Reticulofenestra erbae*, *Reticulofenestra hampdenensis*, *Reticulofenestra lockeri*, *Reticulofenestra reticulata*, and *Reticulofenestra umbilicus*. Medium-sized taxa, such as *Reticulofenestra bisecta* and *Reticulofenestra daviesii*, are also present, whereas small-sized taxa, particularly *Reticulofenestra minuta*, occur only in limited amounts. This assemblage composition indicates a dominance of large-sized *Reticulofenestra* morphotypes over small-sized forms, indicating relatively stable and nutrient-limited surface-water conditions during the NP17 interval in the study area (Table 3).

These findings are consistent with low-latitude Middle–Late Eocene marine settings characterized by enhanced upper-ocean stratification and reduced nutrient supply, conditions that favored the proliferation of larger reticulofenestrid morphotypes (Fokkema et al., 2024; Hutchinson et al., 2021).

### 3.5 Warm-Water Index (WWI)

In all samples assigned to the NP17 interval, the WWI is primarily controlled by the abundance of *Coccolithus pelagicus*, whereas *Reticulofenestra umbilicus* occurs only in limited amounts (Table 4). Elevated contributions of warm-water taxa, particularly *Coccolithus pelagicus*, indicate warm and relatively stable surface-water conditions during the NP17 interval in the Bayat Basin. These conditions are consistent with low-latitude Eocene records characterized by enhanced upper-ocean stratification and reduced nutrient supply (Fokkema et al., 2024).

### 3.6 *Discoaster* Abundance Ratio (DAR)

The *Discoaster* Abundance Ratio (DAR) ranges from 3.7% to 16.6% (Table 5) and shows a progressive increase from the lower to the upper part of the measured section. Samples MR.01–MR.03 (3.7–4.4%) are characterized by relatively limited *Discoaster* representation, whereas samples MR.05 and MR.06 (15.3–16.6%) show a more pronounced contribution of *Discoaster* within the assemblage.

This upward trend indicates a gradual shift in nannofossil composition, reflecting increasing influence of *Discoaster*-producing taxa through time. Such variations suggest changes in surface-water conditions, particularly in relation to water-column structure and ecological stability during deposition.

The persistence and increasing contribution of *Discoaster* throughout the section are consistent with low-latitude Middle–Late Eocene marine records, where nannofossil assemblages commonly reflect stable and stratified surface-water conditions despite broader climatic variability (Fokkema et al., 2024; Westerhold et al., 2024).

### 3.7 Total *Reticulofenestra* Abundance

*Reticulofenestra* constitutes a major component of the assemblage in all samples, indicating its ecological significance within the nanoplankton community during deposition (Table 6). The consistent presence and relatively strong contribution of this genus across the studied interval suggest stable environmental conditions that supported continuous coccolithophore productivity.

Such assemblage characteristics are commonly associated with stratified surface waters, where *Reticulofenestra* forms a dominant component of pelagic carbonate production. The observed distribution pattern therefore reflects relatively stable upper-ocean conditions rather than highly dynamic or strongly upwelling environments.

Table 3. Comparison table of Reticulofenestra as RSR indicators in the study area.

Sample	Small <i>Reticulofenestra</i> (<5 $\mu\text{m}$ )	Medium <i>Reticulofenestra</i> (5-7 $\mu\text{m}$ )	Large <i>Reticulofenestra</i> (>7 $\mu\text{m}$ )	RSR (Small/Large)
MR.01	3	10	12	0.25
MR.02	5	10	12	0.41
MR.03	1	7	13	0.07
MR.04	2	5	12	0.16
MR.05	2	7	9	0.22
MR.06	4	12	18	0.22

Table 4. Abundance table of WWI indicators in the study area.

Sample	<i>C. pelagicus</i>	<i>R. umbilicus</i>	Total Nannofossil	WWI(%)
MR.01	4	0	45	8.9
MR.02	15	1	54	29.6
MR.03	1	0	26	3.8
MR.04	2	0	36	5.6
MR.05	1	0	26	3.8
MR.06	4	0	54	7.4

Table 5. Abundance table of *Discoaster* as DAR indicators in the study area.

Sample	Total <i>Discoaster</i>	Total Nannofossil	DAR (%)
MR.01	2	45	4.4
MR.02	2	54	3.7
MR.03	1	26	3.8
MR.04	3	36	8.3
MR.05	4	26	15.3
MR.06	9	54	16.6

Table 6. Abundance table of Reticulofenestra in the study area.

Sample	Total <i>Reticulofenestra</i>	Total Nannofossil	Percentage (%)
MR.01	25	45	55.5
MR.02	27	54	50
MR.03	21	26	80.7
MR.04	19	36	52.7
MR.05	18	26	69.2
MR.06	34	54	62.9

Based on the integrated interpretation of RSR, WWI, DAR, and total Reticulofenestra abundance, the paleoclimatic conditions of the Bayat Basin during the NP17 interval (Middle–Late Eocene) are interpreted to have been dominated by warm and stratified surface waters. The dominance of medium- to large-sized Reticulofenestra and the consistent presence of *Discoaster* indicate stable upper-ocean structure and limited nutrient input during deposition. (Fokkema et al., 2024; Westerhold et al., 2024).

Although the NP17 interval postdates the peak of the EECO, global syntheses indicate that low-latitude sea-surface temperatures remained relatively elevated during the Middle–Late Eocene despite progressive long-term climatic variability (Westerhold et al., 2024). The nannofossil data from the Bayat Basin, therefore, suggest that southern Java remained under a sustained warm tropical marine influence during this interval.

### 3.8 Implications for Low-Latitude Greenhouse Climate Dynamics

The dominance of large-sized *Reticulofenestra* and the relatively high abundance of *Discoaster* during the NP17 interval indicate that the studied section was deposited under persistently warm and stratified marine conditions. Such assemblage characteristics are typical of low-latitude Eocene environments, where stable surface waters and limited nutrient supply promoted the proliferation of oligotrophic coccolithophore communities. These observations suggest that the Bayat Basin remained under a strong tropical greenhouse influence throughout the Middle–Late Eocene.

Recent syntheses of Middle–Late Eocene climate evolution emphasize that low-latitude ocean systems

maintained relatively elevated sea-surface temperatures and persistent upper-ocean stratification despite long-term global cooling trends (Westerhold et al., 2024). Integrated geochemical and micropaleontological records further demonstrate that tropical plankton communities continued to reflect greenhouse-like surface-water structures even as variability increased in higher-latitude regions (Fokkema et al., 2024; Ma et al., 2024). Such latitudinal differences in climate expression have been linked to enhanced ocean heat storage and reduced seasonal contrast in equatorial regions (Hutchinson et al., 2021).

The paleoclimatic signals obtained from the Bayat Basin are consistent with this broader framework. While several mid-latitude marine records document progressive cooling during the later Eocene (Westerhold et al., 2024), the studied section instead preserves evidence of sustained warm and oligotrophic surface-water conditions. This contrast highlights the relatively stable nature of tropical marine environments during this interval.

These findings contribute to the growing recognition that tropical marine systems did not respond uniformly to global Paleogene cooling. Instead, low-latitude regions appear to have maintained relatively stable greenhouse conditions despite increasing climatic variability elsewhere. This underscores the importance of incorporating Southeast Asian low-latitude records, such as the Bayat Basin, into global paleoclimate syntheses, which are still dominated by mid-latitude datasets from the Atlantic and Pacific oceans.

## 4. Conclusion

Based on nannofossil analysis of the claystone from the Gamping-Wungkal Formation. The distribution of

nannofossil assemblages is dominated by *Reticulofenestra*, *Coccolithus*, and *Discoaster*, with limited occurrences of *Cyclicargolithus* and *Sphenolithus*. The most abundant species include *Reticulofenestra bisecta*, *Reticulofenestra erbae*, *Coccolithus pelagicus*, and *Discoaster barbadiensis*.

Relative age determination based on nannofossil zonation indicates that the studied claystone unit corresponds to the NP17 zone, equivalent to the Middle-Late Eocene.

Paleoclimatic interpretation derived from the *Reticulofenestra* Size Ratio, *Discoaster* Abundance Ratio, Warm-Water Index, and total *Reticulofenestra* abundance suggests that during the NP17 interval, marine conditions were dominated by a warm climate with a relatively stable water column, reflecting the development of the Bayat Basin under tropical greenhouse climate conditions during the Middle-Late Eocene.

#### Acknowledgements

The authors acknowledge the Research and Development Center for Oil and Gas Technology (LEMIGAS) for providing facilities and technical support for SEM sample preparation and analysis in this study.

#### References

- Agnini, C., Fornaciari, E., Raffi, I., Catanzariti, R., Pälke, H., Backman, J., Rio, D., 2014. Biozonation and Biochronology of Paleogene Calcareous Nannofossils from Low and Middle Latitudes. *Newsletters Stratigr.* 47, 131–181.
- Agnini, C., Monechi, S., Raffi, I., 2017. Calcareous Nannofossil Biostratigraphy: Historical Background and Application in Cenozoic Chronostratigraphy. *Lethaia* 50, 447–463. <https://doi.org/10.1111/let.12218>
- Blaj, T., Backman, J., Raffi, I., 2023. Late Eocene to Oligocene preservation history and biochronology of calcareous nannofossils from paleo-equatorial Pacific Ocean sediments. *Riv. Ital. di Paleontol. e Stratigr.* 129, 457–483. <https://doi.org/10.13130/2039-4942/5920>
- Fang, S., Xi, D., Sun, Q., Li, D., 2024. The bivalve-bearing carbonate platform on the east Tethys during the middle Eocene and its response to the Tethys transgression 1–15. <https://doi.org/10.3389/feart.2024.1398474>
- Farida, M., Jaya, A., Ahmad, A., Nugraha, J., 2024. The Eocene to Oligocene boundary and paleoclimatic indications based on calcareous nannofossils of Tonasa Formation, South Sulawesi, Indonesia. *Foss. Rec.* 27, 221–231. <https://doi.org/10.1017/foss.2023.XX>
- Fokkema, C.D., Agterhuis, T., Gerritsma, D., Goeij, M. De, Liu, X., Regt, P. De, 2024. Polar amplification of orbital-scale climate variability in the early Eocene greenhouse world 1303–1325.
- Gallagher, S.J., Auer, G., Brierley, C.M., Fulthorpe, C.S., Hall, R., 2024. Cenozoic History of the Indonesian Gateway. *Annu. Rev. Earth Planet. Sci.* 52, 581–604. <https://doi.org/10.1146/annurev-earth-040722-111322>
- Ghandour, I.M., Balc, R., Faris, M., Helal, S., Mosa, G.A., Aljhdali, M.H., 2023. New Insight into the Middle Eocene Calcareous Nannoplankton Biostratigraphy and Paleoenvironment from Fayoum and Beni Suef Areas, Egypt 129, 343–359.
- Hall, R., 2019. The Plate Tectonics of Indonesia and Surrounding Regions. *Geol. Soc. London, Spec. Publ.* 355, 1–24. <https://doi.org/10.1144/SP355.1>
- Hall, R., 2011. Australia--SE Asia Collision: Plate Tectonics and Crustal Flow, in: Hall, R., Cottam, M.A., Wilson, M.E.J. (Eds.), *The SE Asian Gateway: History and Tectonics of the Australia--Asia Collision*, Geological Society, London, Special Publications. pp. 75–109. <https://doi.org/10.1144/SP355.5>
- Hidayat, E., Muslim, D., Zakaria, Z., Permana, H., Wibowo, D.A., 2021. Tectonic Geomorphology of the Karangsambung Area, Central Java, Indonesia 85–105. <https://doi.org/10.17794/rgn.2021.4.8>
- Hollis, C.J., Naeher, S., Clowes, C.D., Naafs, B.D.A., Pancost, R.D., Taylor, K.W.R., Dahl, J., Li, X., Ventura, G.T., Sykes, R., 2022. Late Paleocene CO<sub>2</sub> drawdown, climatic cooling and terrestrial denudation in the southwest Pacific.
- Hutchinson, D.K., Coxall, H.K., Lunt, D.J., Steinthorsdottir, M., Boer, A.M. De, Baatsen, M., Heydt, A. Von Der, Huber, M., Kennedy-asser, A.T., Kunzmann, L., 2021. The Eocene – Oligocene transition: a review of marine and terrestrial proxy data, models and model – data comparisons 269–315.
- Jatiningrum, R.S., Saputra, R., Phang, G., Sato, T., 2022. Sedimentation rates and calcareous nannofossil biostratigraphy of the Nanggulan Formation, Kulon Progo, Indonesia. *Bull. Mar. Geol.* 37. <https://doi.org/10.32693/bomg.37.1.2022.766>
- Judd, E.J., Tierney, J.E., Huber, B.T., Wing, S.L., Lunt, D.J., Ford, H.L., Inglis, G.N., Mcclymont, E.L., Brien, C.L.O., Rattanasriampaipong, R., Si, W., Staitis, M.L., Thirumalai, K., Anagnostou, E., Cramwinckel, M.J., Dawson, R.R., Evans, D., Gray, W.R., Grossman, E.L., Henahan, M.J., Hupp, B.N., Macleod, K.G., Connor, L.K.O., Luisa, M., Montes, S., Song, H., 2022. The PhanSST global database of Phanerozoic sea surface temperature proxy data. <https://doi.org/10.1038/s41597-022-01826-0>
- Luan, X., Lunt, P., 2021. Journal of Asian Earth Sciences Latest Eocene and Oligocene tectonic controls on carbonate deposition in eastern Java and the south Makassar Straits, Indonesia. *J. Asian Earth Sci.* 220, 104900. <https://doi.org/10.1016/j.jseaes.2021.104900>
- Lunt, D.J., Luan, X., 2023. Cenozoic tectonic reorganization of Southeast Asia and implications for regional paleoclimate. *Glob. Planet. Change* 226, 104097. <https://doi.org/10.1016/j.gloplacha.2023.104097>
- Lunt, P., 2023. Cenozoic Isolated Carbonate Platforms of Southeast Asia, in: *Cenozoic Isolated Carbonate Platforms, SEPM Special Publication. SEPM (Society for Sedimentary Geology)*. <https://doi.org/10.2110/sepmsp.114.06>
- Ma, R., Aubry, M., Bord, D., Jin, X., Liu, C., 2024. Inferred nutrient forcing on the late middle Eocene to early Oligocene (~ 40 – 31 Ma) evolution of the coccolithophore *Reticulofenestra* (order Isochrysidales).
- Menini, A., Mattioli, E., Vinçon-laugier, A., Suan, G., 2021. Paleocene-Eocene Thermal Maximum Pr ub Ar tic Pr eP ub Ar tic. <https://doi.org/10.1127/nos/2021/0621>
- Mulyaningsih, S., 2016. Volcanostratigraphic Sequences of Kebo–Butak Formation at Bayat Geological Field Complex, Central Java Province and Yogyakarta Special Province, Indonesia. *Indones. J. Geosci.* 3, 77–94. <https://doi.org/10.17014/ijog.3.2.77-94>
- Novita, D., Barianto, D.H., Novian, M.I., 2014. Planktonic foraminifera biozonation of the Middle Eocene–Oligocene Kebo Formation, Bayat, Central Java. *Ber. Sedimentol.* 31, 70–78.
- Okada, H., Honjo, S., 1973. The distribution of oceanic coccolithophorids in the Pacific. *Deep Sea Res.* 20, 355–374. <https://doi.org/10.1016/0011->

- Pearson, P.N., Foster, G.L., Wade, B.S., 2015. Atmospheric Carbon Dioxide through the Eocene--Oligocene Climate Transition. *Nature* 461, 1110–1113. <https://doi.org/10.1038/nature08447>
- Raffi, I., Backman, J., Backman, J., 2022. The role of calcareous nannofossils in building age models for Cenozoic marine sediments : a review. *Rend. Lincei. Sci. Fis. e Nat.* 33, 25–38. <https://doi.org/10.1007/s12210-022-01048-x>
- Ratumanan, R.C.F., Isnaniawardhani, V., Muljana, B., 2023. Middle Eocene nannofossil assemblages responding to depositional dynamics of the Elat Formation, Maluku. *J. GeoCelebes* 7, 138–153. <https://doi.org/10.20956/geocelebes.v7i2.25371>
- Samudra, S., Sutisna, K., 1992. Peta Geologi Lembar Klaten, Jawa, Skala 1:100.000.
- Surono, 2009. Litostratigrafi Pegunungan Selatan Bagian Timur Daerah Istimewa Yogyakarta dan Jawa Tengah. *J. Geol. dan Sumberd. Miner.* 19, 209–221.
- Umiyatun, S., Kurniawan, R.E.J., Prastistho, B., Geologi, P.S., Klaten, K., Tengah, J., 2006. Studi Nannofosil Pada Satuan Batulempung Formasi Wungkal-Gamping Lintasan Watuprahu. *Proceeding PIT IAGI* 35, 21–22.
- Villa, G., Persico, D., Florindo, F., others, 2021. Integrated calcareous nannofossil and magnetostratigraphic record of ODP Site 709: Middle Eocene to Oligocene paleoceanography of the equatorial Indian Ocean. *Mar. Micropaleontol.* 169, 102051. <https://doi.org/10.1016/j.marmicro.2021.102051>
- Westerhold, T., Agnini, C., Anagnostou, E., Hilgen, F., Hönisch, B., Pälike, H., Wade, B., Sosdian, S., Kasbohm, J., 2024. Timing Is Everything. <https://doi.org/10.1029/2024PA004932>
- Westerhold, T., Marwan, N., Drury, A.J., others, 2021. An astronomically dated record of Earth's climate and its predictability over the last 66 million years. *Science* (80-. ). 369, 1383–1387. <https://doi.org/10.1126/science.aba6853>



© 2026 Journal of Geoscience, Engineering, Environment and Technology. All rights reserved. This is an open access article distributed under the terms of the CC BY-SA License (<http://creativecommons.org/licenses/by-sa/4.0/>).